Hybrid Controller for a Single Flexible Link Manipulator

Waladin K. Sa'id
Control Systems Dept.
University of TechnologyBaghdad, Iraq
waladinksy@yahoo.com

Bahaa I. Kazem
Mechatronics Eng Dept.
University of Baghdad
bahaak@mit.edu

Alya'a M. Manaty
College of Science
University of Thi-Qar
alyaanow@yahoo.com

Abstract

In this study, the dynamic modeling and step input tracking control of single flexible link is studied. The Lagrange-assumed modes approach is applied to get the dynamic model of a planner single link manipulator. A Step input tracking controller is suggested by utilizing the hybrid controller approach to overcome the problem of vibration of tip position through motion which is a characteristic of the flexible link system. The first controller is a modified version of the proportional-derivative (PD) rigid controller to track the hub position while sliding mode (SM) control is used for vibration damping. Also, a second controller (a fuzzy logic based proportional-integral plus derivative (PI+D) control scheme) is developed for both vibration damping and hub position tracking. A comparison is made between the performances of these two controllers. The Hybrid controller with PD and SM shows better tracking behavior than obtained from the suggested fuzzy $(PI+D)^2$ controller for a single link flexible manipulator.

Keywords: Flexible Link, Single Link, Hybrid Control, Fuzzy Control.

/

الخلاصة

في هذه الدراسة تم دراسة النموذج الديناميكي والسيطرة على حركة ذراع ذو وصلة واحدة single link. تم تطبيق طريقة لاكرانج - النمط الكفوء Lagrange-assumed modes approach للحصول على نموذج ديناميكي لذراع الانسان الآلي. وتم الحصول على نموذج خطي للذراع ذو الوصلة الواحدة والذي تم محاكاته بأستخدام برنامج Matlab وأداة Simulink للتحليل والمحاكاة. تم اقتراح مسيطر لتتبع الادخال من فكرة المسيطر الهجين hybrid controller للتغلب على مشكلة الاهتزاز في طرف الذراع خلال الحركة والذي هو من صفات الهياكل المرنة. حيث تم تصميم نسخة معدلة من مسيطر PD لتتبع مسار المفصل بينما تم استخدام سيطرة النمط المنزلق sliding mode لتخميد الاهتزازات. وكذلك تم تطوير مسيطر ثاني (مسيطر منطق مضبب Fuzzy $(PI+D)^2$) كطريقة للسيطرة على كل من تخميد الاهتزازات وتتبع مسار المفصل. وتمت مقارنة نتائج اداء المسيطرين والتي تظهر بوضوح تفوق عمل المسيطر الهجين من النوع الاول مقارنة مع مسيطر المنطق المضبب المقترح.

1. Introduction

Many of today's robots are required to perform tasks which demand a high level of accuracy in end-effector positioning. Most robots cannot directly sense this position and instead calculate it using the joint angles and forward kinematics equations. This technique assumes that the links connecting the joints are rigid, and thus many robots have large, heavy links which behave like true rigid links. This prevents oscillations in the links which cause errors in the calculated end-effector position. Since the links are heavy, much of the joint motor's power is expended moving the link and holding them up against gravity. Also payloads must be kept quite small compared to the mass of the robot itself, since large payloads will cause sagging and vibrations in the links which create uncertainty in end-effector position. This results in a situation where these rigid robots are very inefficient and slow. In an attempt to solve these problems, the field of flexible robots was created, Natarajan et al (1998).

In order to fully exploit the potential offered by flexible robot manipulator, it is desirable to have an explicit, complete, and accurate dynamic model. This model must consider the effects of structural link flexibility and properly deal with vibrational behavior. Different schemes for modeling of the manipulators are studied by a number or researchers as described below. The mathematical models of the manipulators are generally derived from energy principles and for a simple rigid manipulator, the rigid arms store kinetic energy by virtue of their moving inertia and store potential energy by virtue of their position in the gravitational field, but the flexible arms store potential energy by virtue of the deflections of its links.

To include bending one may often use the Euler-Bernoulli equation which ignores shearing and rotary inertia effects. These two effects may be incorporated using a Timoshenko beam element which generally must be used if the beam is short relative to its diameter, Book et al (1990). In most models of flexible manipulators Euler-Bernoulli beams are used.

The robotic systems with flexible links are continuous dynamical systems characterized by an infinite number of degrees of freedom and are governed by nonlinear coupled, ordinary and partial differential equations. The exact solution of such systems is not feasible practically and the infinite

Dimensional model imposes severe constraints on the design of controllers as well. Hence, they are truncated to some finite dimensional models using assumed modes method (AMM), finite elements method (FEM) or lumped parameters method.

In the literature a number of techniques for deriving equations of motions were used to develop the dynamic equations of motion of flexible link systems. Three main techniques were used by researchers, namely: Newton-Euler approach , Boyer et al (1996), Lagrangian approach , Geniele et al (1997), and Hamiltonian approach ,Benati et al (1991).

The control difficulty of flexible arm is due to the non-collocated nature of the sensor and actuator positions which results in unstable zero dynamics. In other words, the nonlinear system is non-minimum phase. Therefore, the system has an unstable inverse dynamics. The non-minimum phase property makes exact asymptotic tracking of a desired tip trajectory impossible, if one employ causal controllers. Furthermore, the robot should handle a wide variety of payloads, the robustness of the control system becomes very important , talebi et al (1996).

The control strategies considered in this field can be divided into open-loop and closed-loop methods. Open-loop control involves altering the shape of actuator commands by considering the physical and vibration properties of the system. The main source of vibration in the flexible manipulator is the motion itself. Thus, input torque profiles are generated by minimizing input energy at system natural frequencies, so that vibration in the flexible manipulator system is reduced during and after the move. Many types of shaped input strategies are developed on the basis of extracting the energies around the natural frequencies. These are, Gaussian shaped input, low pass filtered torque input and band-stop filtered torque input. While closed-loop control uses measurements of the system states and alters the actuator input in order to reduce the system vibration, Azad et al (2003).

A number of feed-back control strategies have been proposed in the literature for the end-point trajectory tracking in flexible manipulators. Book et al (1975) and Hasting et al (1987), employed linear control theory, while Singh et al (1986), De Luca et

al (1989), and De Luca et al (1991) made use of nonlinear decoupling. They recognized that a multi-link arm could not be controlled based on their approach because of nonlinearities in the dynamics of a multi-link arm.

Tang et al. (2006) focused on tracking control problem of flexible link manipulators. In order to alleviate the effects of nonlinearities and uncertainties, a combined control strategy based on neural network (NN) and the concept of sliding mode control (SMC) was proposed systematically. The chattering phenomenon in conventional SMC is eliminated by incorporated a saturation function in the proposed controller, and the computation burden caused by model dynamics was reduced by applying a two-layer NN with an analytical approximated upper bound, which was used to implement a certain functional estimate. In addition, the Lyapunov analysis can guarantee the signals of closed-loop system bounded and the online NN adaptive laws made the system states converge to the sliding surface.

Alwan et al (2008) suggested the dynamic modele and control; of a robot with single flexible-link with revolute joint, which rotates in the horizontal plane. The dynamic equations are derived using the (assumed mode)/Lagrangian formulation, based on Euler-Bernoulli beam theory. Both the rigid degrees of freedom and the elastic degrees of freedom of the system are treated as generalized coordinate. Although the equations of motion of the system are highly nonlinear and coupled, due to the dynamic model derived in this work takes into account the coupling effects between rigid body motions and elastic deformation. The inverse dynamic method is used to present the Trajectory Control of Flexible Robot Arm; the desired position of the end point of the manipulator is given versus time, and the required joint torques are determined, The main difficulty is that the numerical solution of the inverse dynamic problem of flexible manipulators normally diverges. The computed joint torques can be used as feedforward controls which minimize the work of the feedback controller needed to compensate modeling errors.

In this work several control schemes have been suggested and simulated for step input to possessing interesting nonlinear and non-minimum phase features for one flexible link manipulator.

2- Dynamic Modeling Of A Single Flexible Link

The schematic of a planar single-link flexible manipulator is shown in **Fig. 1**. Where (X , Y) is an inertial coordinate frame, and (x , y) is the coordinate assigned for a flexible link moving with instantaneous Center of Mass (CoM). θ, $w(x,t)$, ℓ, and τ represent the hub angular position, the deflection along the arm, the length of the link, and the torque applied to the hub, respectively.

Single link flexible arm modeled as an Euler-Bernoulli beam in rotation. At one end, the arm is clamped on a rigid hub mounted directly on the vertical shaft of a DC motor, the other end is free to flex in a horizontal plane, and has a mass mp as a payload. It is assumed that the length of the beam, ℓ is much greater than its width, thus restricting the beam to oscillate in the horizontal direction. Neglecting the effects of shear deformation and rotary inertia, the deflection of any point on the beam is given by the Euler-Bernoulli beam equation Thomson (1981).

The Euler-Bernoulli beam theory and the assumed modes method can be used to express the deflection $w(x,t)$ of a point located at a distance x along the link as:

$$w(x,t) = \sum_{i=1}^{n} \phi_i(x)\delta_i(t)$$

(1)

where $\phi_i(x)$ is the mode shape function and $\delta_i(t)$ is the time varying modal function and n is the number of finite modes.

The absolute vector of a point along the link is described by:

$$P = \begin{bmatrix} p_x \\ p_y \end{bmatrix} = \begin{bmatrix} \cos\theta & -\sin\theta \\ \sin\theta & \cos\theta \end{bmatrix} \begin{bmatrix} x \\ w \end{bmatrix}$$

$$= \begin{bmatrix} x\cos\theta & -w\sin\theta \\ x\sin\theta & +w\cos\theta \end{bmatrix}$$

(2)

In order to derive the equations of motion for this system which is a combination of a lumped parameter part (the hub rotation and the payload mass) and distributed parameter part (the link deformation); an energy-based method is the most convenient, i.e. Lagrange formulation. The Lagrangian, L, of the system can be determined by substituting equation for the total kinetic energy and the total potential energy ($L = T - V$).

Therefore, the kinetic energy T and the potential energy V of the system have to be computed.

$$T = T_h + T_\ell + T_p \tag{3}$$

where T_h is the kinetic energy contributions from the hub:

$$T_h = \frac{1}{2} J_h \dot{\theta}(t)^2 + \frac{1}{2} m_h \dot{w}_0^2 \tag{4}$$

Where w_o is the deflection at the hub. From the geometric boundary condition this is equal to zero. T_ℓ from the link: is:

$$T_\ell = \frac{1}{2} \int_0^\ell \dot{p}^{\,t} \dot{p} \; dx \tag{5}$$

Where

$$\dot{p}^t \dot{p} = w^2 \dot{\theta}^2 + x^2 \dot{\theta}^2 + 2xw\dot{\theta} + \dot{w}^2$$

Similarly, the kinetic energy associated with the payload can be written as:

$$T_p = \frac{1}{2} m_p \dot{w}_\ell^2 + \frac{1}{2} J_p \dot{\theta}(t)^2 \tag{6}$$

Where w_ℓ is the deflection at the end of the link

The potential energy of the link is composed of two parts: the gravitational energy V_g, and the strain potential energy V_e owing to the flexure of the link Chapnik et al (1991),

$$V = V_e + V_g \tag{7}$$

Since the movement of the link is assumed in the horizontal plane only, the gravitational energy can be neglected. The potential energy resulting from the elastic deformation of the link is given by:

$$V_e = \frac{1}{2} \int_0^\ell EI \, w''^2 \, dx \tag{8}$$

The potential energy V_e, of the system is stored in the flexible modes and can be attributed to "modal stiffnesses" K which are evaluated by integrals over the length of the link.

Then the dynamic equations of the system can be derived using the Euler-Lagrange. A system with n+1 generalized coordinates q must satisfy n+1 differential equations of the form:

$$\frac{d}{dt}\left[\frac{\partial L}{\partial \dot{q}}\right] - \frac{\partial L}{\partial q} = U \tag{9}$$

The computational details on various differentials and integrals can be found in Manaty

2008, results are a coupled set of second order dynamic equations:

$$M(q_i)\ddot{q}_i + C(q_i,\dot{q}_i) + D\dot{q}_i + Kq_i + g(q_i) = U \tag{10}$$

$$
\begin{bmatrix} M_{rr}(q) & M_{rf}^T(q) \\ M_{fr}(q) & M_{ff}(q) \end{bmatrix}\begin{bmatrix} \ddot{\theta} \\ \ddot{\delta}_i \end{bmatrix} + \begin{bmatrix} C_{rr}(q,\dot{q}) & C_{rf}(q,\dot{q}) \\ C_{fr}(q,\dot{q}) & C_{ff}(q,\dot{q}) \end{bmatrix} +
$$
$$
\begin{bmatrix} d_{rr} & 0 \\ 0 & D_{ff} \end{bmatrix}\begin{bmatrix} \dot{\theta} \\ \dot{\delta}_i \end{bmatrix} + \begin{bmatrix} 0 & 0 \\ 0 & K_{ff} \end{bmatrix}\begin{bmatrix} \theta \\ \delta_i \end{bmatrix} + \begin{bmatrix} g_r(q) \\ g_f(q) \end{bmatrix} = \begin{bmatrix} 1 \\ 0 \end{bmatrix}\tau \tag{11}
$$

where r and f denote rigid and flexible part, respectively. $M(q_i)$ and K_{ff} are the positive definite symmetric inertia matrix and positive definite diagonal stiffness matrix respectively .

The elements ($i=n+1$, $j=n+1$) of the inertia matrix and stiffness matrices for a single link robot with one vibration mode take on the expression below.

$$m_{11}(q) = J_h + J_p + \rho\frac{\ell^3}{3}$$

$$m_{12}(q) = \rho\int_0^\ell x\phi_1 \, dx$$

$$m_{21}(q) = m_{12}^T(q)$$

$$m_{22}(q) = m_p\phi_\ell^2 + m_h\phi_0^2 + \rho\int_0^\ell x\phi_1 \, dx$$

$$k_{22} = EI\int_0^\ell \phi_1''^2 \, dx$$

3. Hybrid Controller

Similarly to most of the contributions in the field, the proposed control method is developed for the one-link flexible arm as a first step towards general multi-link arms. The suggested control approach consists of two sub-controllers; one is slow sub-controller to tracking the desired input, and the other is fast sub-controller to damp out vibration. Using the dynamic model eq. (11) and eq. (12), a hybrid controller is designed. The rigid sub-controller will be built using the inverse control approach (Augmented PD controller), while the flexible sub-controller is sliding mode control (SMC).

3.1 Augmented PD Controller

The purposes of slow sub-controller are tracking input without steady state error and reducing coupling effect from flexibility. To design the control u_r for the n joint coordinates q_r, infinitely stiff links are assumed. The rigid body model for the manipulator can be recovered from the n upper rows of eq. (12), by setting $q_i = 0$ for all (n_e)flexible links. This yields $q_e = \dot{q}_e = \ddot{q}_e = 0$, and the equations of motion are then

$$M_r(q_r)\ddot{q}_r(t) + C_r(q_r, \dot{q}_r) + g_r(q_r) = u_r \tag{12}$$

Accurate measurements of joint variables, either angles or displacements and joint velocities are assumed to be available. If the tip location r_t of the manipulator is of interest, then

$$r_t = f(q_r) \tag{13}$$

the vector of desired joint coordinates q_r^d must be computed using the inverse kinematic equation

$$q_r^d = f^{-1}(r_t^d) \tag{14}$$

The well-known inverse dynamics control method is chosen here, where the control u_r is taken to be a function of the manipulator state in the form;

$$u_r = M_r(q_r)\overline{u}_r + C_r(q_r, \dot{q}_r) + g_r(q_r) \tag{15}$$

Because the mass matrix M_r is invertible, the combined system reduces to

$$\ddot{q}_r = \overline{u}_r \tag{16}$$

where u_r represents a new input vector, which is still to be chosen, for the system.
The approach

$$\overline{u}_r = -K_p q_r - K_D \dot{q}_r + r \tag{17}$$

with constant control matrices K_P and K_D leads to a simple linear second-order system,

$$\ddot{q}_r + K_D \dot{q}_r + K_p q_r = r \tag{18}$$

where r is the reference input. Under the assumption of positive definite matrices K_P and K_D, this system is asymptotically stable. Given a desired trajectory q_r^d, one may choose

$$r = \ddot{q}_r^d + K_D \dot{q}_r^d + K_p q_r^d \tag{19}$$

The tracking error $e = q_r^d - q_r$ then satisfies the homogeneous second-order differential equation

$$\ddot{e} + K_D \dot{e} + K_p e = 0 \tag{20}$$

Choosing K_P and K_D as diagonal gain matrices of the type

$$K_p = diag\{\omega_1^2 ......\omega_n^2\}$$
$$K_D = diag\{2\delta_1\omega_1 ....2\delta_n\omega_n\} \tag{21}$$

results in a closed-loop system that is globally decoupled. Each joint response is equal to the response of a second-order system characterized by a natural frequency ω_i and a damping ratio δ_i.

The method of inverse dynamics is attractive because the nonlinear coupled dynamics of the manipulator is canceled and replaced by n linear decoupled second-order systems. However, such exact cancellation schemes leave open many issues of sensitivity and robustness due to unavoidably imperfect compensation. These issues are addressed in several books dealing in details with modeling and control of robot manipulators, e.g. Spong et al 1989. However the final control law used in this paper is given by

$$u_r = M_r(q_r)\overline{u}_r + K_r(q_r, \dot{q}_r) + g_r(q_r) \tag{22}$$

$$\overline{u}_r = \ddot{q}_r^2 + K_D(\dot{q}_r^d - \dot{q}_r) + K_p(q_r^d - q_r) \tag{23}$$

3.2 PI - Sliding Mode Controller (SMC)

The flexible sub-controller should be designed to damp out vibration. Sliding Mode Control (SMC) is often favored as a basic control approach, especially because of its insensitivity property toward the parametric uncertainties and the external disturbances. SMC are characterized by control laws that are discontinuous on a certain manifold in the state space, the so-called sliding surface. The control law is designed such that the representative point's trajectories of the closed-loop

system are attracted to the sliding surface and once on the sliding surface they slide towards the origin . However the major drawback in the SMC approach is the undesired phenomenon of chattering because of the discontinuous change of control laws across the sliding surface. In practical engineering systems, chattering may cause damage to system components, as well as excite unmodeled and high frequency plant dynamics , Kwatny et al (1987).

There exist several techniques to eliminate chattering. PI-SMC approach provides an effective way to resolve the chattering problem. In general, the first step to illustrate the standard SMC is to define a time-varying sliding surface, S(t), that is linear and stable. The S(t) acting on the tracking-error expression selected in this work, is:

$$S(t) = \lambda e(t) + \dot{e}(t) \qquad (24)$$

where λ is a strictly positive constant, and $e(t)$ is the tracking error, while $\dot{e}(t)$ is the time derivative of the tracking error e(t). Since the aim of this controller is to damp out the vibration to zero, therefore $q_f(t)$ and $\dot{q}_f(t)$ are used instead of e(t) and $\dot{e}(t)$ respectively, then eq. 24) becomes

$$S(t) = \lambda q_f(t) + \dot{q}_f(t) \qquad (25)$$

Sliding mode means that once the state trajectory has reached the sliding surface $S(e, \dot{e}) = 0$ the system trajectory remains on it while sliding into the origin (0,0), independently of model uncertainties, unmodeled frequencies, and disturbances, Quang (2000).

To keep the $S(e, \dot{e})$ at zero, the control law is designed to satisfy the following sliding condition (Lyapunov function):

$$V = \frac{1}{2} S(t)^T S(t) \ge 0 \qquad (26)$$

Its time derivative becomes $\dot{V} = \dot{S} S$ and the control u_f is chosen such that

$$\dot{S}(t) S(t) \le -\eta |S(t)| \qquad (27)$$

where η is a positive constant that guarantees the system trajectories hits the sliding surface in a finite

time. Essentially, eq. (26) states that the squared "distance" to the surface, as measured by $S^T S$, decreases along all system trajectories. Thus, eq. (27) provides a sufficient reaching condition such that the tracking error e_i will asymptotically converge to zero, Quang (2000). In order to meet that condition, the control law is chosen as follows

$$u_f = -K_s \, \text{sgn}(S) \qquad (28)$$

where the sliding gain $K_s > 0$ and sgn(S) is a sign (or signum) function, which is defined as

$$\text{sgn}(S) = \begin{cases} -1 & if \ S < 0 \\ 0 & if \ S = 0 \\ 1 & if \ S > 0 \end{cases} \qquad (29)$$

As explained before, using a sign function often causes a chattering problem. A proportional-integral combination of the sliding function is proposed in a boundary layer in place of the signum function by Quang (2000). This continuous controller can force the system states to reach the sliding surface and attain high tracking performance. The equation for this saturated proportional-integral functions is given by

$$\rho_{PI}(\sigma_{PI}) = \begin{cases} 1 & if \ \sigma_{PI} > 1 \\ \sigma_{PI} + K_I \int_{t_{i0}}^{t_i} \sigma_{PI} & if \ -1 \le \sigma_{PI} \le 1, \\ -1 & if \ \sigma_{PI} < -1 \end{cases} \qquad (30)$$

where

$$\sigma_{PI} = \frac{S}{\Phi};$$

where $K_I > 0$ is an integral gain, and t_{i0} is the initial time when the system states enter the boundary layer $B(t)$ which is defined as ,Nguyen et al (2003),

$$B(t) = \{e, |S(e,t)| \le \Phi\}, \Phi > 0 \qquad (31)$$

where $|S(x,t)|$ is the distance between state e and sliding surface S, Φ is the boundary layer thickness.

If $|\sigma_{PI}| \ge 1$ the integration term in eq. (30) will be reset to zero to prepare for the system state entering boundary layer. It is assumed that the

chosen integration gains K_I are sufficiently large such that

$$\dot{\sigma}_{PI} + K_I \sigma_{PI} > 0 \quad for\ all\ \sigma_{PI} > 0$$

$$\dot{\sigma}_{PIi} + K_I \sigma_{PI} < 0 \quad for\ all\ \sigma_{PI} < 0 \tag{32}$$

Inequalities (33) imply that ρ_{PI} increases for all $\sigma_{PI} > 0$, and ρ_{PI} decreases for all $\sigma_{PI} < 0$ Nguyen et al (2003).

The overall Fuzzy PI +D control system is shown in **Fig. 2**.

Similar to the classical (PI+D) controller which uses two integrators, the fuzzy $(PI + D)^2$ control approach uses two fuzzy (PI + D) controllers. The first controller is used for set-point tracking control, while the second one is used for vibration damping. The block diagram of this approach is shown in **Fig. 3.**

Eight rules, " D output" had been used for fuzzy control output. The formulation for these rules is given by Tang et al (2001).

5. Simulation Results And Discussion

The simulation results for a robotic system that has single link with one mode are discussed. The numerical model used in the simulations is illustrated below. It is derived by using the assumed modes method with clamped-free shape functions presented in section 2. The link parameters are given in **Table 1**, these parameters are taken from Azad et al (2003). One mode shape approximation is used for this example. The inertia M, stiffness K, and damping D matrices, are obtained by using the Matlab program given in Manaty (2008).

$$M = \begin{bmatrix} 1.5623 & 0.1837 \\ 0.1837 & 0.3910 \end{bmatrix}$$

$$D = \begin{bmatrix} 0 & 0 \\ 0 & 0.1 \end{bmatrix} \quad K = \begin{bmatrix} 0 & 0 \\ 0 & 31.6931 \end{bmatrix}$$

The simulation results of a single link with one mode approximation using controllers (the hybrid and the fuzzy $(PI+D)^2$) designed in section 3 and 4

4. The Fuzzy $(Pi+D)^2$ Controller

This approach was proposed by Soorasksa et al 1998, to control the flexible link manipulator. The overall fuzzy PI+D control law can be obtained by algebraically summing the fuzzy PI control law and the fuzzy D law together. The result is

$$u_{PID}(nT) = u_{PI}(nT - T) + K_{uPI}\Delta u_{PI}(nT) +$$
$$u_D(nT - T) - K_{uD}\Delta_{uD}(nT) \tag{33}$$

to track a step reference input are shown in Fig.s 4 and 5.

In this simulation, gains for the hybrid controller are chosen as (K_P=5 and K_D = 5) for augmented controller. While the gains for the SMC (λ = 10, ϕ = 0.1, K_I = 10, K_S= 4).

A (1 radian) step reference is applied to the hybrid controller, as well as the fuzzy $(PI+D)^2$ controller (with K_P = 4000 and K_D = 800 for rigid part and K_P = 4000 and kD = 600 for flexible part).

The proposed hybrid controller demonstrates a significant improvement over the other controller (fuzzy $(PI+D)^2$) as illustrated in **Fig. 4**. The manipulator tracks the step reference trajectory with almost no overshoot or undershoots. The hybrid controller has better settling time (2.5 sec) and has virtually no ripple.

The fuzzy $(PI+D)^2$ controller results show that there is small oscillations in the transient response causing the step response to reach steady-state in (4.7 sec). The fuzzy controller has slightly longer settling time 3.5 sec.

The control signal for the rigid link and for the flexible mode is shown in **Fig. 8** while the tracking error signal is shown in **Fig. 6**. Both results show that the two controllers approaches give unequal torque values for the rigid link and for the deflection as shown in **Fig. 7**. It can be noticed that the error system with hybird controller reaches zero steady state error after a few seconds (3 sec) while system response when using the fuzzy (PI+D)2 controller there is (0.1) steady state error.

6. Conclusions

In this paper, a model for the single flexible-link manipulator which describes both linear and nonlinear behavior of the entire system has been developed.

Two approaches to control the flexible link manipulator are used. The first one is a hybrid (PD and sliding mode) controller. Where, the augmented PD controller is used as a hub position control while the sliding mode control is used to damp out the vibration of tip position. The second control approach is to use a fuzzy $(PI+D)^2$ controller for both, the hub angle control and tip deflection control.

The hybrid controller has a steady state error which reaches zero in a fast manner and gives good tracking to the trajectory while the fuzzy $(PI+D)^2$ has a small steady state error when both controllers try to track the step reference input.

The control torque signal for the hybrid controller shows higher initial torque and lower mean value torque signal than that using fuzzy $(PI+D)^2$.

In general the hybrid controller shows better behavior than the proposed fuzzy $(PI+D)^2$ controller for the single flexible link manipulator.

References

Alwan A. Adel, Kazem I. Bahaa, Hussein T. Mustafa "Modeling and Trajectory Control of Planar Flexible Robot Arm", UOB Journal of applied and pure scinces, Vol. 15 No.4, pp. 1818-1826, 2008.

Azad, A. K. M., Tokhi M. O., and Anand N. , "Teaching of Control for Complex Systems Through Simulation," Proceedings of the 2003 ASEE/WFEO International Colloquium, American Society for Engineering Education, 2003.

Benati, M., and Morro A., "Formulation of Equations of Motion for a Chain of Flexible Links Using Hamilton's Principle," ASME Journal of Dynamic Systems, Measurements, and Control, vol. 116, pp. 81-88, 1994.

Book, W. J., "Modeling, Design, And Control Of Flexible Manipulator Arms: A Tutorial Review," Proceedings of the 29th IEEE Conference on Decision and Control, pp. 500-506, Dec. 1990.

Book, W.J., Maizz-Neto O., and Whitney D.E., "Feedback Control of Two Beam, Two Joint Systems with Distributed Flexibility," ASME

Journal of Dynamic Systems, Measurements, and Control, vol. 97, pp. 424-431, 1975.

Boyer, F., and Coiffet,P. "Generalisation Of Newton-Euler Model For Flexible Manipulators," Journal of Robotic Systems, vol. 13, no. 1, pp. 11-24, 1996.

Chapnik, B. V., Heppler G. R., and Aplevich J. D., "Modeling Impact On A One-Link Flexible Robotic Arm," IEEE Transactions on Robotics and Automation, vol. 7, no. 4, August 1991.

De Luca, A., and Siciliano B., "Closed-Form Dynamic Model Of Planar Multilink Lightweight Robots," IEEE Transactions on Systems, Man, and Cybernetics, vol. 21, no. 4, pp.826-839, 1991.

De Luca, A., Lucibello P., and Ulivi G., "Inversion Techniques For Trajectory Control Of Flexible Robot Arms," Journal of robotic systems, vol. 6, no. 4, pp. 325-344, 1989.

Geniele, H., Patel R. V., and . Khorasani K, "End-Point Control Of A Single Link Flexible Manipulator: Theory And Experiments," IEEE Transactions on Control Systems Technology, vol. 5, no. 6, 556-560, 1997.

Hastings, G. G., and Book W. J., "A Linear Dynamic Model For Flexible Robot Manipulators," IEEE Control Systems Magazine, pp. 61-64, February 1987.

Kwatny, H. G., and Siu T. L., "Chattering in Variable Structure Feedback Systems," Proceedings of IFAC 10th World Conference, vol. 8, pp. 307-314, 1987.

Manaty, A. M., "Hybrid Controller For A Flexible Link Robot Manipulator", Ph.D. thesis, University of technology, control and systems dept., Nov. 2008.

Natarajan, K., Yu S., and Karray F., "Modeling And Control Design For A Flexible-Link Manipulator" IEEE Canadian Conference on Electrical and Computer Engineering, vol. 1, pp. 117-120, issue 24-28 May 1998.

Nguyen, T. V. M., Ha Q. P. and Nguyen H. T., "A Chattering-Free Variable Structure Controller for Tracking of Robotic Manipulators," Faculty of Engineering, University of Technology, Sydney, 2003.

Quang, N. H., "Robust Low Level Control of Robotic Excavation," Ph.D., Thesis, Australian Centre for Field Robotics, University of Sydney, Mar. 2000.

Singh, S. N., and Schy A. A., "Control of Elastic Robotic Systems by Nonlinear Inversion and Modal Damping," ASME Journal of Dynamic Systems, Measurements, and Control, vol. 108, pp. 180-189, 1986

Sooraksa, P., and Chen G., "Mathematical Modeling and Fuzzy Control of a Flexible-Link Robot Arm," Mathematical Computation and Modelling, vol. 27, no. 6, pp. 73-93, 1998.

Spong, M. and Vidyasagar M., "Robot Dynamics and Control," McGraw-Hill, 1989.

Talebi, H. A., "Neural Network-Based Control of Flexible-Link Manipulators," Ph. D. thesis, Concordia University, Montréal, Québec, Canada, 1997.

Tang K. S., Man K. F. , Chen G. and Kwong S, " An optimal fuzzy PID controller", IEEE Transaction on industrial Electronics , Vol.48, No. 4, pp 757-765, Aug. 2001.

Tang, Y., Sun F., Sun Z., "Neural Network Control Of Flexible-Link Manipulators Using Sliding Mode," Neurocomputing, no. 70, pp. 288–295, 2006.

Thomson, W. T., "Theory Of Vibration With Applications," Prentice-Hall Inc., Englewood Cliffs, N. J., 2nd edition. 1981.

List of Symbols

$e(t)$	Tracking error
EI	Flexural rigidity (N.m^2)
J	Total inertia (kg.m^2)
J_h	Hub inertia (kg.m^2)
J_P	Payload inertia (kg.m^2)
K	Stiffness matrix
K_D	Derivative gain
K_S	Sliding gain
K_I	Integral gain
K_p	proportional gain
K_{UPI}	PI constant control gain
L	Lagrangain
l	Length of the link (m)
M	Inertia matrix
m_l	Mass of the link (kg)
m_p	Mass of the payload (kg)
P	Position vector of any point along the link
q	Generalized coordinate
$\dot{q}_r$	Velocity of the rigid part
$\dot{q}_r^d$	Desired velocity of joint coordinate
r	Position vector of link end
$S(t)$	Time-varying sliding surface
T	Kinetic energy
T_l	Kinetic energy for link
T_h	Kinetic energy for hub
T_p	Kinetic energy for payload
u_f	Control signal for flexible part
u_r	Control signal for rigid part
V	Potential energy
V_e	Potential energy due to elasticity
V_g	Potential energy due to garvity
$w_i(x,t)$	Deflection of a point x along the ith link
w_l	Defection at tip position (m)
θ	Joint position of the link (degree)
φ	Eigen function of the link
δ	Flexible mode of the link
$\theta_c(t)$	Position of the center of mass
ρ	Mass density (kg/m)
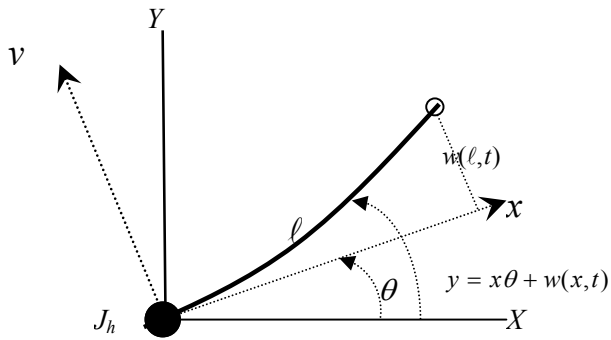
Fig. 1 Single Flexible Link Manipulator

Table 1 The Link parameters for simulation of manipulator, Azad et al 2003

Parameter	Value	Units
Length	1.22	m
Mass density	0.24	kg/m
Flexural rigidity	11.82	$N \cdot m^2$
Hub mass	2	kg
Hub moment of inertia	1.35	$Kg \cdot m^2$
Payload mass	0.045	Kg
Payload inertia	0.067	$Kg.m^2$
damping	0.1	__
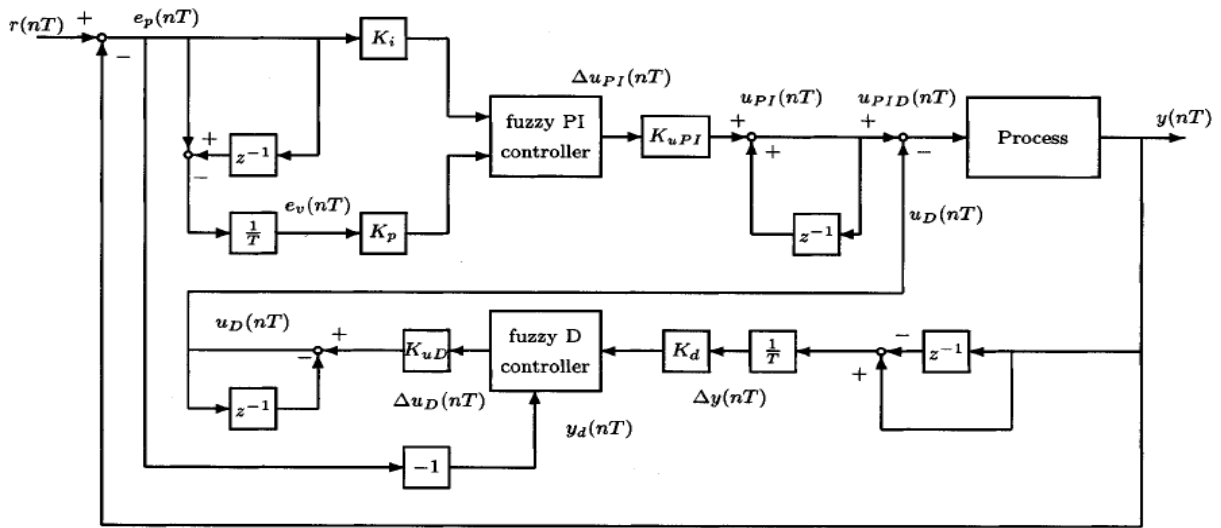
Fig. 2   Fuzzy PI+D control system Sooraksa et al 1998.
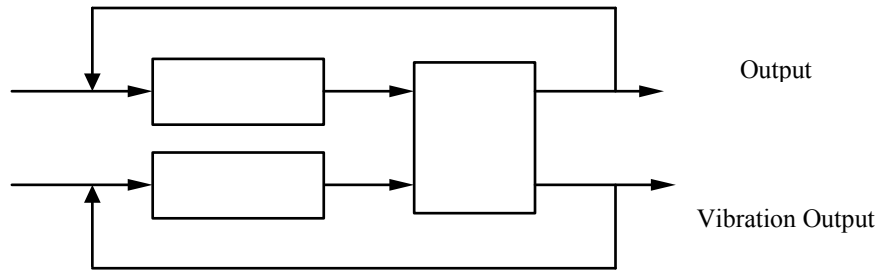
Fig. 3 The fuzzy (PI+D)^2 control approach Sooraksa et al 1998.
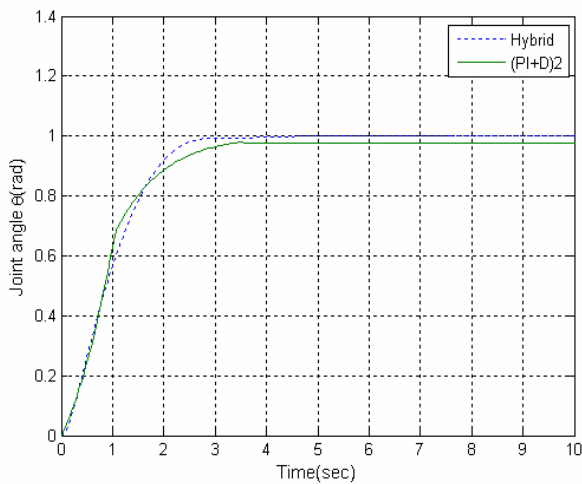
(a) Tracking position
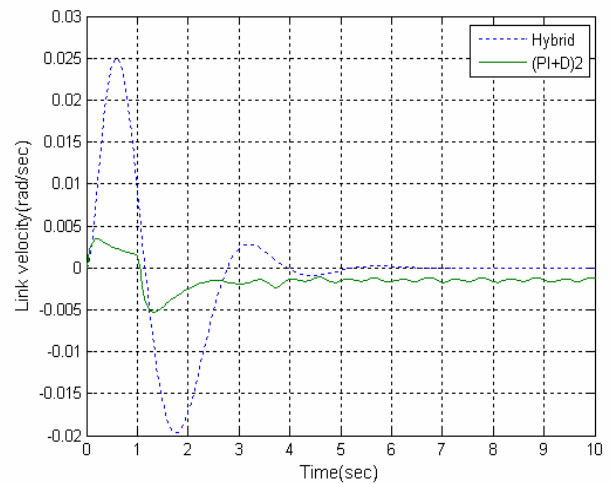
(b) Tracking velocity

Fig. 4 Comparison of tracking performance of hybrid and fuzzy (PI+D)^2 controllers.

Fuzzy PI+D
Controller

Fuzzy PI+D
Controller
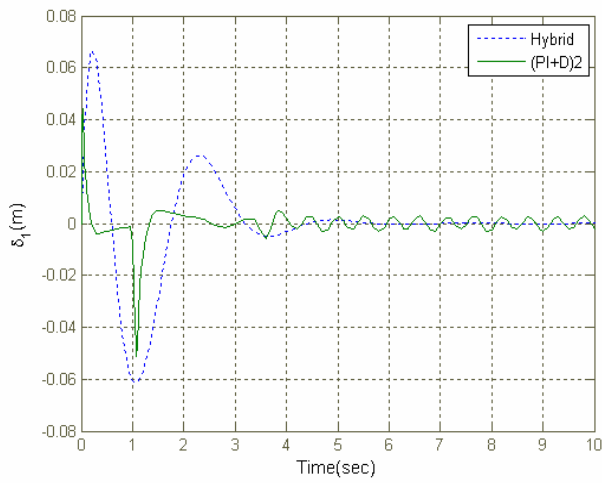
(a) Tip deflection position
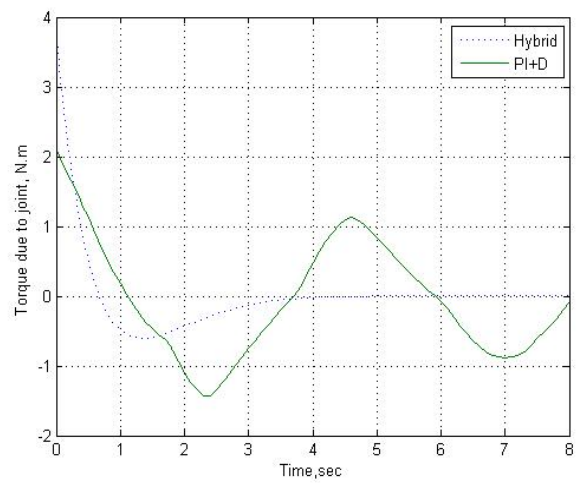
(a) Control torque signal for the rigid part.
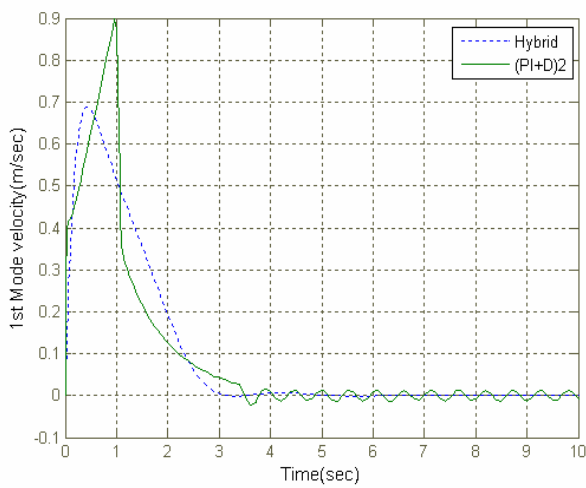
(b) Tip deflection velocity

Fig. 5 Comparison of first mode suppression performance of hybrid and fuzzy $(PI+D)^2$ controllers.
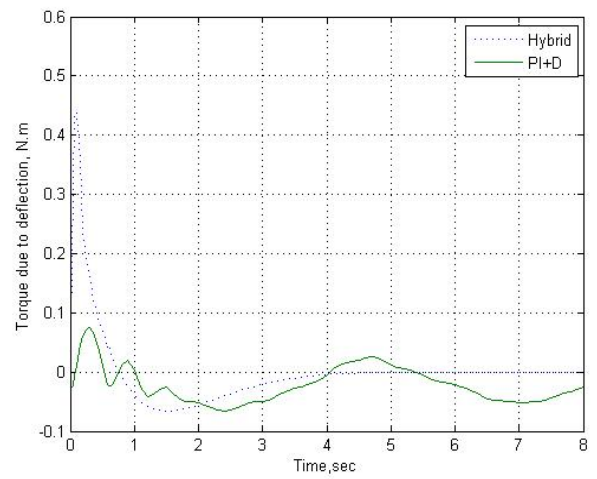
(b) Control torque signal for the flexible part.

Fig. 6 Control torque signal of hybrid and fuzzy $(PI+D)^2$ controllers.
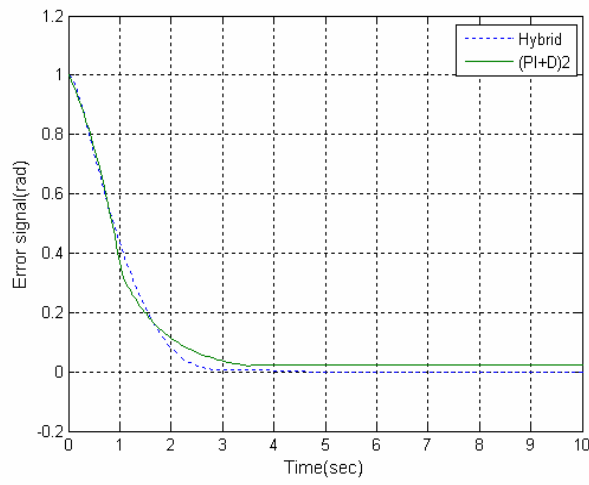
(a) Rigid part error signal.
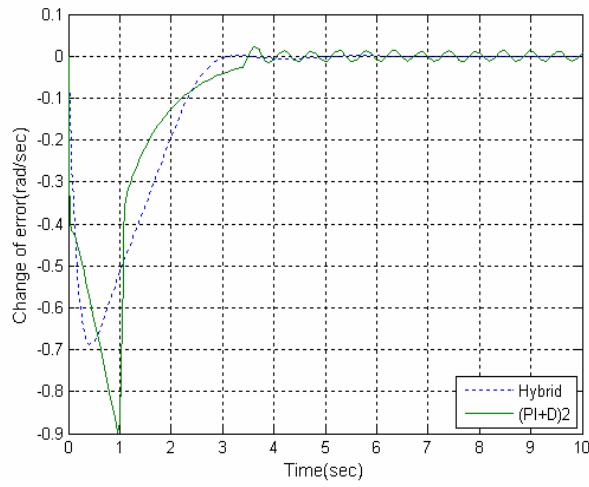
(b) Flexible part error signal.

Fig. 7 Tracking error signals.